Hyperpycnal river flows from an active mountain belt

Simon Dadson,[1,2] Niels Hovius,[1] Stuart Pegg,[1] W. Brian Dade,[3] M. J. Horng,[4] and H. Chen[5]

Received 29 September 2004; revised 21 July 2005; accepted 22 August 2005; published 3 December 2005.

[1] Rivers draining the tectonically active island of Taiwan commonly discharge suspended sediment to the ocean at hyperpycnal concentrations (>40 kg m^{-3}), typically during typhoon-driven floods. During the period 1970–1999, between 99 and 115 Mt yr^{-1} of sediment was discharged at hyperpycnal sediment concentrations from Taiwan to the sea. This amount represents 30–42% of the total sediment discharge from Taiwan to the ocean. The spatial distribution of hyperpycnal discharge broadly mirrors the pattern of total sediment discharge, and rivers draining catchments having recent earthquakes and weak rocks, such as the Choshui and Erhjen, discharge up to 50–70% of their sediment at hyperpycnal concentrations. Following the Chi-Chi earthquake, the frequency of hyperpycnal flows increased, because of an earthquake-driven increase in sediment supply. Landslides triggered by the Chi-Chi earthquake have resulted in an increase in the concentration of suspended sediment in rivers for a given water discharge. In turn, the threshold flood discharge required to generate hyperpycnal flow has decreased, and so hyperpycnal flows are occurring more frequently. Our findings suggest that if hyperpycnal plumes evolve into bottom-hugging gravity currents descending to and ultimately debouching in the deep sea, earthquakes may be recorded as bundles of turbidites.

Citation: Dadson, S., N. Hovius, S. Pegg, W. B. Dade, M. J. Horng, and H. Chen (2005), Hyperpycnal river flows from an active mountain belt, *J. Geophys. Res.*, *110*, F04016, doi:10.1029/2004JF000244.

1. Introduction

[2] The marine sedimentary record is a convolution of geomorphic sediment supply and transport processes which, once understood, may reveal important information on the palaeoclimate and palaeoseismicity of terrestrial source regions [*Hovius and Leeder*, 1998]. Understanding the link between terrestrial source and seafloor sink is particularly important for tectonically active, mountainous regions, from which more than half of the total suspended sediment supplied by rivers to the sea originates [*Milliman and Syvitski*, 1992].

[3] The aim of this paper is to investigate the long-term significance of flood discharge to the delivery of sediment to the ocean from Taiwan, with a particular focus on flood-generated plumes that are notably denser than seawater. Taiwan is an ideal location for such a study, as it is characterized by high erosion rates (3–6 mm yr^{-1}) resulting from rapid plate convergence (80 mm yr^{-1}) accompanied by frequent large earthquakes including the 1999 M_w 7.6 Chi-Chi earthquake, and a vigorous subtropical climate with an average of four typhoons per year [*Dadson et al.*, 2003].

[4] In the following sections, we present calculations of the total amount of suspended sediment discharged from Taiwan at hyperpycnal concentrations and examine the recurrence interval of hyperpycnal flows in the 30-year hydrometric record. We then consider the effect of the Chi-Chi earthquake, which mobilized a large amount of sediment in headwater catchments, on the frequency and magnitude of hyperpycnal plume formation. The paper concludes with a discussion of the fate of hyperpycnal plumes and considers information about past erosional, climatic, and tectonic processes that may be extracted from any resulting marine deposits.

2. Background

[5] The fate of sediment-laden river water discharged into a coastal ocean is determined by its overall density relative to the density of the ambient seawater. The following terms were defined by *Bates* [1953]. River discharge is defined as hypopycnal if the density of the debouching plume is less than that of the receiving seawater. In this case, the sediment will form a spreading plume at the sea surface and will gradually settle to the seabed as hemipelagite. The river discharge is described as homopycnal if its density is equal to that of the receiving seawater, in which case the plume will mix vertically with the seawater and may drop its load in a mouth bar. If the river plume density is greater than that of the receiving seawater, the flow is hyper-

[1]Department of Earth Sciences, University of Cambridge, Cambridge, UK.
[2]Now at Centre for Ecology and Hydrology, Wallingford, UK.
[3]Department of Earth Sciences, Dartmouth College, Hanover, New Hampshire, USA.
[4]Water Resources Agency, Ministry of Economic Affairs, Taipei, Taiwan.
[5]Department of Geoscience, National Taiwan University, Taipei, Taiwan.

0148-0227/05/2004JF000244$09.00

pycnal. In this case the plume will sink to the seafloor and may form a turbidity current. Alternatively, if it is marginally hyperpycnal, the plume may descend to a level of neutral buoyancy and lift off the gently sloping seafloor, to form a deep-sea hemiturbidite deposited from a spreading nepheloid layer at mid-level depths [*Stow and Wetzel*, 1990]. Hyperpycnal plumes are a particularly important source of terrigenous sediment to the ocean and may form a significant mechanism for carbon sequestration in deep ocean basins. A hyperpycnal flow can erode the seafloor over which it travels and, over geologic time, many such flows may form a canyon incising the continental margin.

[6] It is possible to define a critical sediment concentration above which a river plume will be hyperpycnal. The density of a sediment-laden plume depends on the densities of its fluid and solid parts and on the concentration of sediment in the plume. The density of seawater depends primarily on its temperature and salinity, and secondarily on the amount of sediment already suspended in the coastal ocean. The critical suspended sediment concentration for a plume to become hyperpycnal therefore depends primarily on the prevailing climate and ocean circulation pattern in the region of interest at the time of deposition. *Mulder and Syvitski* [1995] have calculated critical, hyperpycnal values of sediment concentrations of 36–43 kg m^{-3} for various climates, although recent laboratory experiments have shown that hyperpycnal plumes may result from convective instabilities at sediment concentrations as low as 1 kg m^{-3} [*Parsons et al.*, 2001].

[7] Upon entering the ocean, a hyperpycnal plume can result in a sediment-laden gravity current that sinks to the seafloor and may deposit turbidites. The geometry of the resultant turbidite will depend on the topography of the region of deposition. In an unconstrained basin, a laterally spreading fan may form. Alternatively, in a deep-sea canyon the deposit would be confined to the channel, although a lobe may form in the wider, distal reaches. Examples of each in the Taiwan region, with which we are concerned here, include the Choshui Fan in western Taiwan [*Chen*, 1998] and the Kaoping Canyon offshore of southern Taiwan [*Yu et al.*, 1991], respectively. After deposition, turbidites may be modified by seabed processes. Turbidites may be eroded or amalgamated by offshore mass wasting and transport by ocean currents. The original layered structure may be modified by bioturbation and compaction. None of these postemplacement alterations will be considered in this paper, although it is recognized that they may place limits on the resolution at which the stratigraphic record can be interpreted.

[8] Several recent studies have documented hyperpycnal river discharges in rivers draining active mountain belts. *Warrick and Milliman* [2003] estimated that 75% of the cumulative suspended sediment load of the Santa Clara River, California, was transported at hyperpycnal sediment concentrations, and that much of the hyperpycnal discharge occurred on only 30 days in their 50-year record. *Milliman and Kao* [2005] showed that during Typhoon Herb, which swept across Taiwan between 31 July and 1 August 1996 about 80% of the suspended sediment load of several rivers in western Taiwan was delivered at hyperpycnal concentrations. *Mulder et al.* [2001] correlated flood-generated turbidity currents in the Var Canyon, southeast France, with turbidite sequences cored at 2-km water depth in the Mediterranean and showed that, during the past 100 years, 13–14 hyperpycnal turbidity currents were recorded. They calculated that 68–71% of the local, deepwater sedimentary column was deposited by hyperpycnal turbidity currents; 3–6% resulted from slide-induced turbidity currents; and 26% consisted of hemipelagites. We conclude from this brief review of the literature that earthquake- and storm-driven increases in the supply of sediment from rivers to the ocean are likely to be strongest in young, tectonically active mountain belts such as Taiwan, where sediment-laden rivers draining steep landslide-prone landscapes discharge large amounts of sediment directly to ocean basins.

3. Study Location

[9] Taiwan is the product of oblique collision between the Luzon Arc, on the Philippine Sea plate, and the Eurasian continental margin (Figure 1a). Crustal shortening at 80 mm yr^{-1} [*Yu et al.*, 1997] is accompanied by frequent large earthquakes, including the M_w 7.6 Chi-Chi earthquake in 1999. Taiwan has a subtropical climate with an average of four typhoons per year [*Wu and Kuo*, 1999] and mean precipitation of 2.5 m yr^{-1}. Up to 80% of the water discharge occurs during the typhoon season between June and October [*Water Resources Agency of Taiwan*, 1970–2003] (for data see http://gweb.wra.gov.tw/wrweb, September 2004). Typhoons themselves may be ~100 km across although precipitation is generally strongest in the eye wall region and in areas where the flow of air is forced upward as the typhoon circulation interacts with topography [*Lin et al.*, 2002]. Typhoons originate with approximately equal frequency from the north (32%), east (27%), and south (23%) of the island; the remaining 18% of typhoons originate from the southwest, but there is no resulting asymmetry in the pattern of mean annual precipitation [*Wu and Kuo*, 1999]. The combination of active tectonic and climatic regimes leads to erosion rates averaging 3–7 mm yr^{-1} and locally up to 60 mm yr^{-1} [*Dadson et al.*, 2003], driven by fluvial bedrock incision [*Hartshorn et al.*, 2002], landsliding [*Hovius et al.*, 2000], and debris flows [*Lin et al.*, 2004]. Between 1970 and 1998, Taiwan supplied an estimated 384 Mt yr^{-1} of suspended sediment to the ocean [*Dadson et al.*, 2003]. This amount represents 1.9% of the total 20 Gt yr^{-1} global discharge of sediment to the ocean from 0.02% of the continental earth surface [*Milliman and Syvitski*, 1992].

[10] Rivers draining the eastern flank of Taiwan deliver sediment to the Huatung Basin (Figures 1a and 1b), which is up to 5 km deep and makes up the westernmost corner of the Philippine Sea floor. The Huatung Basin contains up to 3 km of sediment, which is derived from the Taiwan orogen [*Malavieille et al.*, 2002]. The basin is bordered by the Gagua Ridge to the east, by the Yaeyama Ridge to the north, and by the Luzon Arc to the south (Figures 1a and 1b). These barriers prevent orogenic sediment escaping to the West Philippine Basin, except through a narrow channel to the north of the Gagua Ridge. Three major rivers on the east coast deliver sediment to the Huatung Basin through sub-

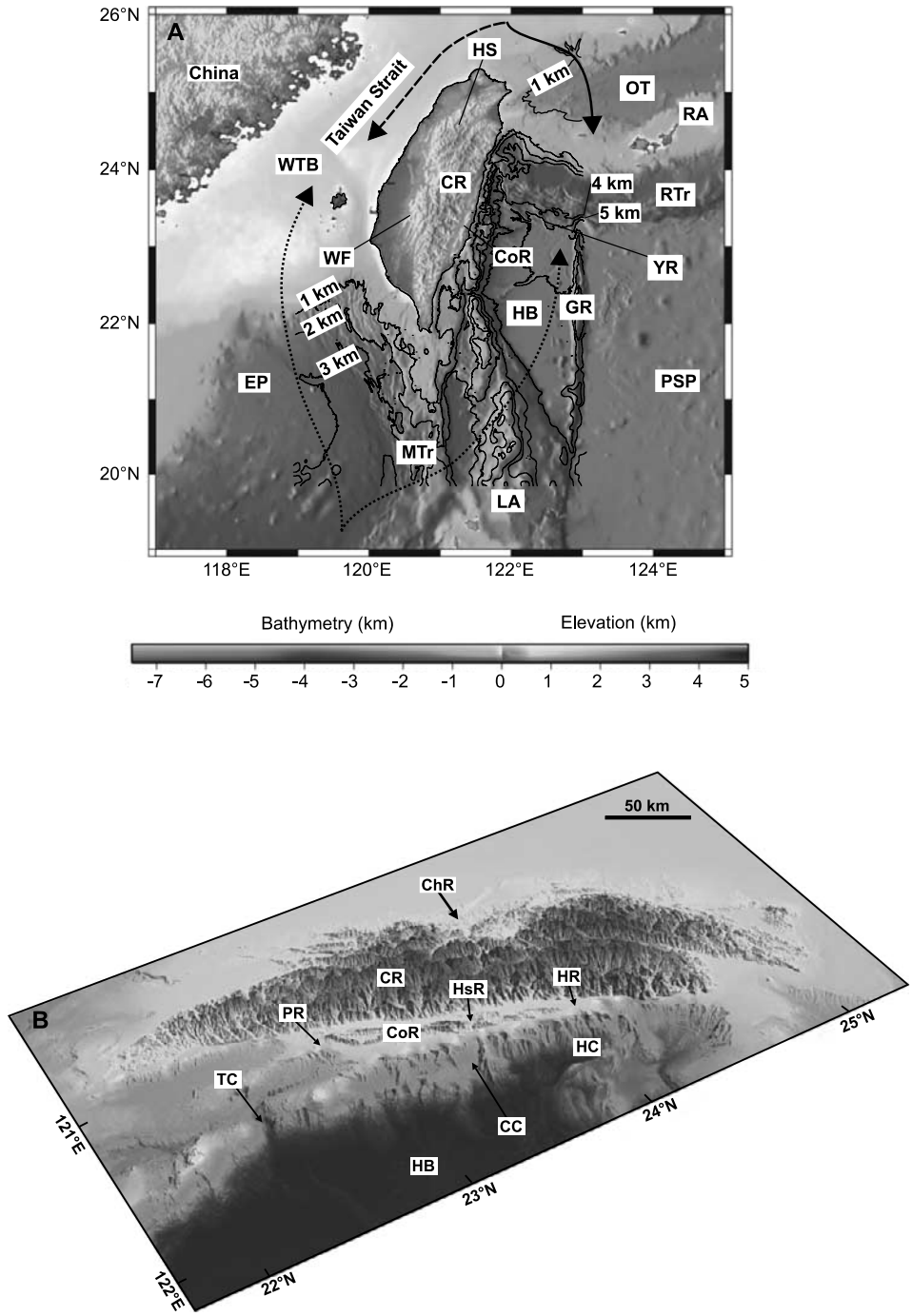

Figure 1. (a) Topography and bathymetry of Taiwan. Bathymetry is from *Liu et al.* [1998]. Definitions are EP, Eurasian plate; PSP, Philippine Sea plate; MTr, Manila Trench; RTr, Ryukyu Trench; OT, Okinawa Trough; WTB, West Taiwan Basin; CR, Central Range; HS, Hsuehshan Range; WF, Western Foothills; CoR, Coastal Range; LA, Luzon Arc; RA, Ryukyu Arc; HB, Huatung Basin; GR, Gagua Ridge; and YR, Yaeyama Ridge. Dotted line is Kuroshio current; solid line (summer) and dashed line (winter) show China coastal current. (b) River-fed submarine canyons off the east coast of Taiwan. Bathymetry is from *Liu et al.* [1998]. Definitions are ChR, Choshui River; HsR, Hsiukuluan River; PR, Peinan River; HR, Hualien River; CC, Chimei Canyon (arrow points to sediment apron); and TC, Taitung Canyon. Contour interval is 1 km.

marine canyons: the Hualien River through the Hualien Canyon; the Hsiukuluan River through the Chimei Canyon; and the Peinan River through the Taitung Canyon (Figure 1b). The Hualien and Taitung canyons are major incised conduits with deep-marine continuations as far east as the northern tip of the Gagua Ridge (Figure 1a). Unlike the other two canyons, the Chimei Canyon is filled with sediment that forms an 8–9 km wide, smooth apron on the canyon floor.

Seismic profiles show that this fill is at least 1 km thick [*Malavieille et al.*, 2002].

[11] Rivers that drain the western flank of Taiwan flow across a coastal plain which is 20–40 km wide into the West Taiwan Basin of the Taiwan Strait (Figure 1a). The West Taiwan Basin developed approximately 6.5 Myr ago by lithospheric flexure of the Chinese continental margin in front of migrating thrust and fold loads in the Taiwan orogenic belt [*Lin and Watts*, 2002]. The basin is occupied by shallow sea (up to 150 m deep) and was subaerially exposed during the late Pleistocene, when the East China Sea was up to 140 m below its present level [*Boggs et al.*, 1979]. In the late Pleistocene, a river (the ancestral Minchiang) is inferred to have flowed southward from mainland China through what is now the Taiwan Strait, where it was probably joined by the nascent Choshui River of Taiwan, via the Penghu Canyon, to the Manila Trench [*Boggs et al.*, 1979]. The Penghu Canyon remains the principal conduit for southward sediment export from the West Taiwan Basin to the deep ocean. The Kaoping River delivers sediment to the Kaoping Canyon, which also extends over 240 km to the Manila Trench.

[12] Sea temperature and salinity dictate the threshold suspended sediment concentration in otherwise freshwater river discharge for the formation of hyperpycnal plumes. The temperature of the sea around Taiwan changes not only in response to seasonal changes in air temperature and wind patterns, but also in response to changes in ocean currents. The sea surface temperature in the open water to the east of Taiwan is approximately 28°C in summer and 24°C, in winter; water temperature remains approximately constant with depth in the uppermost 80 m, and declines linearly thereafter to 6°C at 1,000 m [*Boggs et al.*, 1979]. In the shallower water of the Taiwan Strait, the summer sea surface temperature is about 29°C, which is maintained to a depth of 20 m and declines steadily to 18°C at 150 m depth; in winter the surface temperature is approximately 23°C in the uppermost 80 m and declines steadily to about 16°C at 150 m depth. The Kuroshio Current carries high-salinity water (about 35‰) from the Philippines to Taiwan, which ensures that the salinity of seawater in the region remains at approximately 34 ± 0.8‰. For such conditions, *Mulder and Syvitski* [1995] give a critical hyperpycnal sediment concentration range at the surface of 36–39 kg m^{-3}. In summer, the threshold may be as low as 36 kg m^{-3} at the surface; in winter it may reach 43 kg m^{-3} in deep water. In this paper, a critical sediment concentration of 40 kg m^{-3} is used. It is possible that high discharges of freshwater into the sea following extreme monsoonal rains or typhoon-generated floods would decrease the salinity of the seawater around Taiwan and therefore decrease the critical sediment concentration required for the formation of a hyperpycnal plume. To our knowledge, there are no available constraints on the rate at which seawater and fresh water are mixed in this region, so we assume that the results obtained using our adopted critical threshold are conservative estimates.

[13] The offshore fate of river plume sediments is partly determined by the northeast and southwest monsoon drift currents, the Kuroshio Current and the China Coastal Current [*Boggs et al.*, 1979]. The main flow of the Kuroshio Current comes from northeast of the Philippines and runs northward along the east coast of Taiwan (see Figure 1a). To the east of Taiwan, the Kuroshio Current is 110–150 km wide, and its axis shifts between 50 and 150 km offshore. The China Coastal Current comes from northern China and moves south along the continental coast. During the winter (September–April) northeasterly winds prevail and this current enters the Taiwan Strait. However, in summer (May–August) the southwest monsoon diverts this current eastward and it cannot enter the Taiwan Strait. The observed pattern of surface ocean currents shows a year-round current to the north-northeast at a velocity of 0.6–1.0 m s^{-1} along the east coast of Taiwan, and a seasonally reversing current at a velocity of 0.4–0.6 m s^{-1} along the west coast of Taiwan that is directed toward the northeast in the summer and the southwest in the winter [*Boggs et al.*, 1979]. Fluvial suspended sediment supplied to the marine basins around Taiwan may be evacuated from its point of initial deposition by sediment transport in ocean currents or submarine mass movement. Lack of high-resolution geophysical and sedimentological sampling of the seafloor in western Taiwan means that little is known about the fate of sediment discharged from rivers on the west coast of Taiwan. However, the lack of muddy sediment on the western Taiwan shelf suggests that a significant proportion of the mud-rich river load is ultimately moved to the deep sea by the strong currents described above. Strong currents in the Taiwan Strait also mobilize medium-coarse sand, and asymmetric sand waves off western Taiwan (around 24°N) indicate southward bed load transport [*Boggs*, 1974]. In contrast, off the east coast of Taiwan, the deep canyons and accumulated sediment in the Huatung Basin suggest that channelized turbidity currents have been frequent and persistent.

4. Methods

[14] To estimate hyperpycnal sediment loads in Taiwan rivers, we have used measurements of water and sediment discharge at 31 coastal hydrometric stations on 29 rivers [*Water Resources Agency of Taiwan*, 1970–2003]. At each hydrometric station, continuous measurements of river stage were made using an automatic stage recorder. Water discharge was calculated from measurements of stage, using an empirically calibrated relation. This relation was recalibrated every six months using resurveyed channel cross sections and measurements of flow velocity [*Water Resources Agency of Taiwan*, 1970–2003]. Suspended sediment concentration was measured with an average frequency of 32 ± 7 times per year using a USDH–48 suspended sediment sampler. Reported measurements of suspended sediment concentration represent the mean concentration of three depth-averaged samples spaced equally along the channel cross section [*Water Resources Agency of Taiwan*, 1970–2003]. An example of the recorded data for the Peinan River 1970–2000 is given in Figure 2. The total suspended sediment discharge can be calculated from these intermittent measurements using several methods, and most commonly based on the development of a rating curve [*Cohn*, 1995]. Here we examine the usefulness of two related but subtly contrasting methods [*Dadson*, 2004]: (1) an average of measured suspended sediment discharges corrected monthly for time-of-sampling bias and (2) a rating curve.

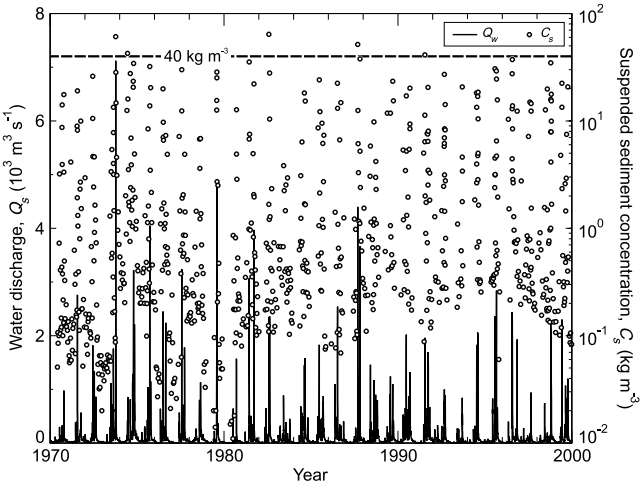

Figure 2. Example of hydrometric data for Peinan River at Taitung Bridge (station 2200H011). Solid line shows water discharge in 10^3 m^3 s^{-1}; circles show suspended sediment concentration in kg m^{-3}. Dashed line indicates 40 kg m^{-3} hyperpycnal density threshold.

[15] Calculating a monthly average of suspended sediment discharge is inappropriate for calculating the amount of sediment discharged during an individual hyperpycnal flow event, which lasts between hours and days, not months. Nevertheless, it is possible to identify individual events that have hyperpycnal suspended sediment concentrations, and to compute the proportion of sediment discharge that these events represent. This approach is the most conservative because it uses only measured data. However, the result is likely to underestimate the total hyperpycnal load because some hyperpycnal events will not have been sampled and many events that were sampled will not have been measured over their entire duration, or at their peak.

[16] An alternative method is to use an empirical rating curve between suspended sediment concentration, C_s, and water discharge, Q:

$$C_s = \kappa Q^b, \tag{1}$$

where κ is sediment concentration associated with unit discharge and b is an exponent with a value typically in the range 0.5–1.0. The main advantage of the rating curve is that each day's sediment discharge receives equal consideration; there is no bias associated with sampling. In practice, a correction is required to account for systematic downward bias introduced when the rating curve parameters are estimated using the method of least squares with a log transform. The problem is easily seen from a consideration of the residuals of log-transformed regression, ε_i, defined as the differences between each observed value and its prediction, $\varepsilon_i = Y_i - \hat{Y}_i$. Residuals of the regression between $X(=\ln(Q))$ and $Y(=\ln(Q_s))$ are normally distributed. The expected value of the residual distribution is zero, indicating that, on average, there is no difference between predicted and observed values. However, when the model prediction or its parameters are back transformed, the regression residuals are no longer normally distributed, and their expected value is usually less than zero. On average, there is therefore a negative difference between predicted and observed values, which can lead to a significant underestimate of river loads. The appropriate procedure for correcting this bias using a minimum variance statistical estimator is described by *Cohn* [1995]. In spite of our adoption of the minimum variance estimator, the rating curve estimates of suspended sediment loads in rivers were on average 63% lower than independent, bathymetrically surveyed rates of sediment deposition in twelve water reservoirs across Taiwan. In contrast, the suspended sediment loads calculated from monthly averages were only 30% lower than those measured from reservoir fill, a discrepancy that may be accounted for by the deposition of bed load in the reservoirs (see *Dadson* [2004] for detailed calculations). Nevertheless, our investigation revealed that the rating curve and monthly average methods produced results that were in linear proportion, which suggests that the minimum variance rating curve method may still offer an accurate assessment of the proportion of sediment discharge that is hyperpycnal even though the absolute estimates are biased downward.

[17] One reason for the consistent underestimation of suspended sediment loads by rating curve methods in Taiwan may be that the daily water discharge data do not capture much of the flashiness of the natural system that would be present if water discharge were recorded more frequently. To assess this, hourly data were obtained for selected floods. The effect of more frequent sampling on the result of the calculation results from the nonlinearity in the rating curve (equation (1)) and can be seen from the following example, which illustrates the effect of Typhoon Toraji on the Choshui River. Over the course of 30 July 2001, the day of the typhoon's peak, the maximum recorded discharge was 28,000 m^3 s^{-1} and the daily mean discharge was 7790 m^3 s^{-1}. The peak suspended sediment concentration was 169 kg m^{-3} and the appropriate rating curve was $C_s = 0.1012\ Q_w^{0.82}$. Application of this rating curve to the daily mean discharge gives a daily mean suspended sediment concentration of 157 kg m^{-3} and a mean suspended sediment discharge of 106 Mt d^{-1}. In contrast, using the same rating curve with the hourly water discharge data presented in section 8 gives a daily mean suspended sediment discharge of 175 Mt d^{-1}, which is higher by 65%.

5. Hyperpycnal Sediment Delivery

[18] Both methods outlined in section 4 were used to obtain estimates of the total sediment discharge delivered to the sea at hyperpycnal concentrations (Table 1) and these values were expressed as a fraction of the total suspended sediment discharge to the sea. All 29 coastal rivers for which more than 8 years of data are available were included in the analysis. Coastal rivers with no measured or predicted hyperpycnal flow are listed in Table 2. In order to exclude the effects of the 1999 Chi-Chi earthquake, which will be discussed later, the data presented in Table 2 are based on recorded measurements between 1970 and the end of 1998. This interval included only one large earthquake, in 1986, which had magnitude M_w 6.5 but was >20 km deep and occurred 20 km off the east coast at Hualien.

Table 1. Estimates of Amount and Proportion of Hyperpycnal Discharges Observed in Major Coastal Rivers Between 1970 and 1998 Calculated Using Rating Curve and Direct Average Methods[a]

	Station Number	Drainage Area, km^2	Length of Discharge Record, years	Number of Sediment Observations	Average of Measured Data				Rating Curve Prediction			
					DPY HP	Total Q_s Mt yr^{-1}	HP Q_s Mt yr^{-1}	HP, %	DPY HP	Total Q_s Mt yr^{-1}	HP Q_s Mt yr^{-1}	HP, %
Watershed												
Fengshan	1290H002	208	31.0	424	0.06	1	0.05	7	0.00	0.12	0	0
Taan	1400H009	633	31.0	709	0.03	7	4	61	0.00	2	0	0
Tachia	1420H035	417	15.0	138	0.07	1	0.12	12	0.00	0.46	0	0
Choshui	1510H058	2,989	14.7	392	0.07	54	28	53	0.27	34	8	24
Pachang	1580H005	441	31.0	366	0.03	6	2	37	0.00	3	0	0
Tsengwen	1630H010	1157	12.0	171	0.00	25	0	0	0.58	23	8	33
Erhjen	1660H009	175	21.5	341	0.89	47[b]	35	64	7.06	21	20	93
Peinan	2200H011	1,584	31.0	850	0.16	88	18	20	0.42	26	8	32
Hsiukuluan	2370H017	1,539	31.0	304	0.00	22	0	0	0.16	18	5	28
Hualien	2420H024	1,506	31.0	307	0.06	31	14	44	0.87	28	17	61
Hoping	2500H003	553	26.0	667	0.12	15	11	73	3.16	40	33	83
Lanyang	2560H006	821	31.0	978	0.06	17	1	8	0.00	9	0	0
Total for hyperpycnal rivers		12,023				297	115	39		205	99	48
Total for gauged area of Taiwan		22,527				384	115	30		234	99	42

[a]Definitions are DPY, days per year; HP, hyperpycnal; and Q_s, suspended sediment discharge.
[b]Direct average is given rather than bias-corrected average (30 Mt yr^{-1}) which is used in calculation for total line of table.

[19] Twelve rivers produced observed and/or predicted hyperpycnal flow during the period of observation. For each of these rivers, Table 1 gives the number of days per year on which hyperpycnal flow was observed and the number of days on which the rating curve model predicts hyperpycnal flow. Figure 3 shows the total observed hyperpycnal sediment discharge of all coastal rivers in Taiwan for which at least one hyperpycnal concentration was observed. The total area from which hyperpycnal discharges occurred was 12,023 km^2, which represents 53% of the total gauged area and 33% of the total area of Taiwan. Within this area, the average suspended sediment erosion rate computed using the monthly average method was 9.3 mm yr^{-1}. No hyperpycnal discharge was recorded or predicted in 17 rivers draining a total area of 10,504 km^2, within which the average suspended sediment erosion rate computed using the monthly average method was 3.1 mm yr^{-1}.

[20] The rating curve model usually predicts more hyperpycnal events than were observed; this is probably due to undersampling of hyperpycnal flows in the observed hydrometric record. The total annual hyperpycnal sediment discharge to the ocean during the period 1970–1999 was 115 Mt yr^{-1}, according to the available observations. This amount represents 30% of Taiwan's total sediment discharge to the ocean (384 Mt yr^{-1}). Both the amount and proportion are likely to be conservative estimates because of undersampling of high flows. In contrast, the rating curve method indicates that 99 Mt yr^{-1} of sediment was delivered under hyperpycnal conditions. This amount is lower than that estimated from direct observations, but represents a higher proportion (42%) of the total suspended sediment discharge estimated using the rating curve method (234 Mt yr^{-1}). In some cases the discrepancies between observed and predicted results are due to

Table 2. Rivers Having No Recorded or Predicted Hyperpycnal Sediment Load Between 1970 and 1999

	Station	Drainage Area, km^2	Number of Sediment Observations	Sediment Discharge (Average) Q_s, Mt yr^{-1}	Sediment Discharge (Rating Curve) Q_s, Mt yr^{-1}
Watershed					
Tanshui[a]	1140H058	842	889	1.0	0.2
Tanshui[a]	1140H066	751	914	1.8	–
Tanshui[a]	1140H067	204	923	1.7	0.2
Nankang	1180H002	122	546	0.1	0.0
Touchien	1300H017	499	330	1.5	0.3
Chungkang	1340H006	165	427	1.6	0.7
Houlung	1350H012	472	488	2.9	0.4
Wu	1430H025	1,981	920	9.8	3.0
Peikang	1540H009	597	961	2.2	1.8
Potzu	1550H003	289	252	2.1	0.7
Chishui	1590H012	227	958	1.8	1.0
Yenshui	1650H006	146	839	1.1	0.4
Kaoping	1730H026	3,076	657	49.0	15.0
Tungkang	1740H002	175	952	0.4	0.2
Linpien	1760H004	310	950	3.3	1.1
Taimarli	2150H003	190	470	0.4	1.5
Chihpen	2170H001	166	865	3.6	0.9
Nanao	2510H005	170	784	2.4	1.5
Shuang	2620H002	122	525	0.0	0.1
Total		10,504		86.7	29.0

[a]This river has three coastal stations.

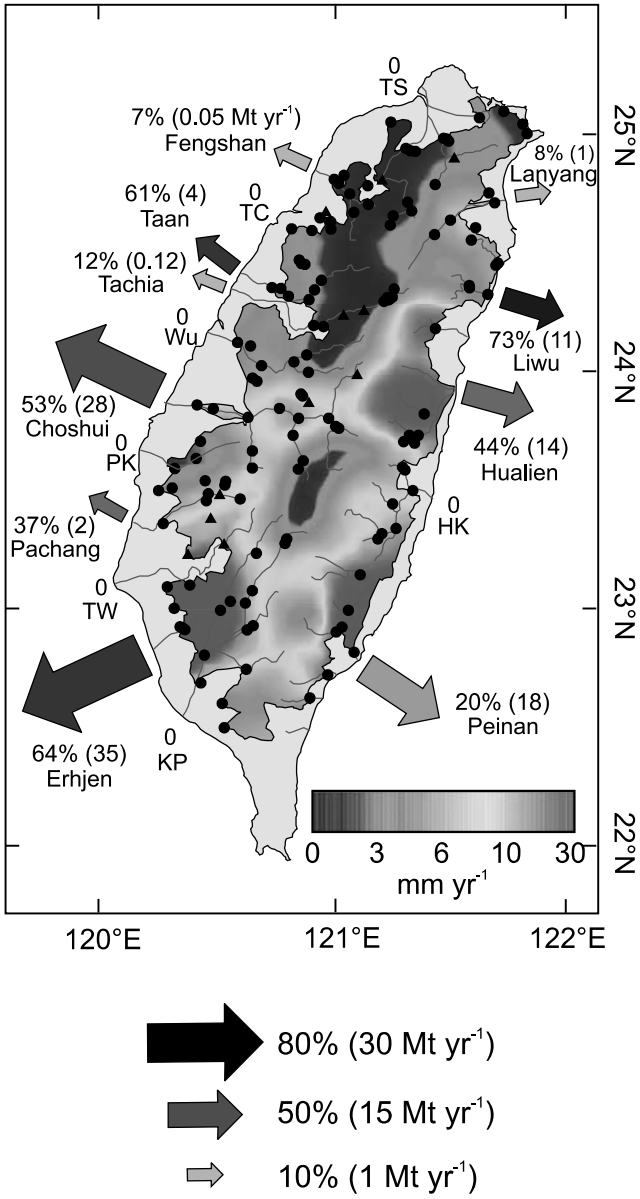

Figure 3. Hyperpycnal discharges to the ocean from Taiwan 1970–1998 based on measured hydrometric data. The map shows decadal average erosion rates for reference [from *Dadson et al.*, 2003]. Arrows indicate rivers for which at least one hyperpycnal discharge was measured (Table 1). The size of each arrow is proportional to the annual average hyperpycnal sediment discharge to the ocean (also given in parentheses); its shade is proportional to the percentage that the hyperpycnal amount represents of the total annual sediment discharge (see legend). These estimates are probably conservative, because they are based on measured data only. River names are given beneath arrows. Rivers labeled "0" had no recorded hyperpycnal sediment discharge between 1970 and 1998. The names of these rivers are abbreviated as follows: TS, Tanshui; TC, Touchien; PK, Peikang; TW, Tsengwen; KP, Kaoping; and HK, Hsiukuluan. Circles indicate hydrometric stations used to construct the erosion map; triangles indicate locations of water supply reservoirs. No data are available in the outermost light grey area. See color version of this figure at back of this issue.

the consistent underprediction of sediment discharge using the rating curve method [*Dadson*, 2004]. In other cases, the discrepancy between observed and predicted results is due to the weaker influence of sampling bias on the rating curve estimates. Water discharge was measured on all days, and so each day is accorded equal consideration in the calculation of sediment load. Departures from this pattern include the Hoping River, for which the rating curve predicted higher overall and hyperpycnal sediment discharge than was observed, and the Choshui River for which the rating curve underpredicted both total and hyperpycnal suspended sediment discharge. We conclude that hyperpycnal sediment discharges in Taiwan between 1970 and 1999 were at least 99–115 Mt yr^{-1}, and represent at least 30–42% of the total sediment discharge from Taiwan to the ocean.

[21] The spatial distribution of hyperpycnal discharge broadly mirrors the pattern of total sediment discharge [*Dadson et al.*, 2003], although there are important differences. The Erhjen and Choshui rivers deliver the largest amount of sediment to the sea at hyperpycnal concentrations. Both of these rivers drain the Western Foothills fold-and-thrust belt, which consists of poorly consolidated mudstones and conglomerates, although the Choshui has its headwaters in stronger metasediments. The Erhjen River, in southwest Taiwan, drains the area of greatest seismic activity in the past 100 years. Southwestern Taiwan is also an area of highly variable runoff and has the highest decadal erosion rate [*Dadson et al.*, 2003]. The Hoping River, on the east coast of Taiwan, is notable for the large hyperpycnal proportion of its total suspended load. Rivers draining the north and northwest of Taiwan have low total hyperpycnal loads. In general, the proportion of their load that these rivers discharge at hyperpycnal concentrations is also low. One exception may be the Taan River, which discharged 61% (4 Mt yr^{-1}) of its load at hyperpycnal concentrations, according to our measurement-based estimate. This exception does not emerge in the corresponding estimates based on a rating curve; indeed, for this river the rating curve estimate indicates no hyperpycnal events at all.

[22] Rivers with no hyperpycnal discharge accounted for 87 Mt yr^{-1} (23%) of the total hypopycnal suspended sediment discharge from Taiwan to the ocean. These rivers mainly drain northwestern Taiwan, although there are notable exceptions such as the Kaoping River in southern Taiwan.

[23] On the east coast, there is an interesting match between deep, incised submarine canyons and rivers with measured hyperpycnal sediment discharge. The Peinan and Hualien rivers both have canyons, and both discharge 20–40% of their load at hyperpycnal concentrations (Figure 3). In contrast, the Hsiukuluan River, which has created a wide sediment apron within the Chimei Canyon, has a lower overall erosion rate and has had no recorded hyperpycnal flow (although a modest amount (5 Mt yr^{-1}) is predicted by the rating curve). Further speculation about any process link that may account for the coincidence between hyperpycnal plumes and offshore canyons is beyond the scope of the present paper.

[24] In summary, the spatial pattern of sediment delivery from Taiwan to the ocean corresponds to the orogen-wide

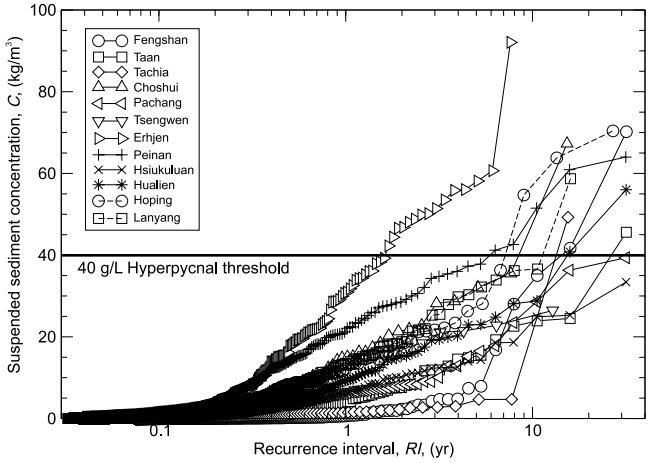

Figure 4. Recurrence interval of hyperpycnal sediment concentration in major coastal rivers that regularly discharge hyperpycnal flows to the ocean. Figure 4 shows measured data only.

pattern of erosion, which indicates that the rate at which suspended sediment is delivered to the ocean is in proportion to the rate of mountain erosion. The rivers with the highest sediment discharge are Peinan, Choshui, and Kaoping. The rivers that discharge the most sediment at hyperpycnal sediment concentrations are Erhjen, Choshui, and Peinan. The rivers that deliver the greatest proportion of their load at hyperpycnal concentrations are Hoping, Erhjen, Taan, and Choshui. The spatial pattern of hyperpycnal sediment discharge broadly mirrors that of erosion rate. Hyperpycnal sediment delivery almost always coincides with large typhoons.

6. Recurrence Interval for Hyperpycnal Flow

[25] In addition to the amount and proportion of sediment discharged by each river to the ocean at hyperpycnal concentrations, we consider the frequency at which hyperpycnal discharges occurred. The recurrence interval of a given measured concentration, C_i can be calculated as

$$R_i = \frac{T+1}{N_i}, \tag{2}$$

where R_i is the recurrence interval (in years) of the ith observation, T is the length of the record (in years), and N_i is the rank of the ith observation (the C_i are ranked in descending order with the maximum assigned $N = 1$).

[26] Figure 4 shows recurrence intervals for sediment concentration in the major coastal rivers that regularly discharge hyperpycnal plumes. The general form of the recurrence plots is exponential, and is driven by the frequency distribution of typhoons but moderated by the erodibility of the catchment substrate. Plots are constructed using observed data rather than rating curve data because the former provides information on the recurrence interval of hyperpycnal flow, while the latter is simply a function of water discharge. Estimates may therefore be biased downward if hyperpycnal events are not sampled, or upward if the same event is sampled on successive days. Inspection of the hydrometric record indicates that the latter is rare and we have not screened the data for this effect. The Erhjen River has the shortest recurrence time (1–2 yr), which is consistent with the fact that this river has a very high specific sediment yield and hyperpycnal load fraction. Other rivers, such as the Peinan, Choshui, and Hoping rivers produce a hyperpycnal discharge approximately every 6–10 years.

7. Extrapolation

[27] Since the 30-year record does not capture the full behavior of the system at longer timescales, we have extrapolated the long-term proportion of sediment supplied by rivers to the ocean using a power law model with realistic constraints on the maximum event size. The long-term average proportion of suspended sediment discharge that is delivered at hyperpycnal concentrations can be computed from the probability distribution of sediment discharge and the suspended sediment rating curve. The probability distribution of sediment discharge describes the relative rate of occurrence of river sediment discharges and can be used to investigate whether the effects of large but rare floods outweigh the cumulative effects of smaller, more frequent floods [e.g., *Wolman and Miller*, 1960]. If the magnitude-frequency distribution can be robustly defined from the available data, then the proportion of sediment discharged above a given concentration can be computed and the factors that control the proportion of hyperpycnal sediment discharge can be examined. The model is defined generally, and then applied specifically to the Choshui River in central west Taiwan. Note that the analysis presented below considers 24-hour discharges, rather than event discharges, although in practice the two are approximately equivalent since most events (e.g., 86% of events in the Choshui River) lasted for less than or equal to 1 day.

[28] In Taiwan, the magnitude-frequency distribution of daily average sediment discharges can be described by a power law of the form:

$$p(Q_s) = uQ_s^{-\alpha-1}, \tag{3}$$

where $p(Q_s)$ is the probability density of measured sediment discharge, Q_s, and u and α are positive constants [*Hovius et al.*, 2000]. Figure 5 shows the probability distribution of suspended sediment discharge for Choshui River, and illustrates that the maximum likelihood estimate of the exponent $\alpha = 0.49$ for suspended sediment discharges greater than 1×10^4 t d^{-1}. There is a rollover for discharges less than 1×10^4 t d^{-1}, which is probably due to censoring of observations lower than this magnitude in the observational record. The slight deviation from the power law at high magnitudes probably results from the finite length of the available record. Parameters of the probability distributions for suspended sediment discharge in other rivers in Taiwan are given in Table 3. The parameter α describes the relative importance of large suspended sediment transport events. This parameter differs between catchments according to hydrological regime and lithology; the latter controls the availability of sediment at low and high flow.

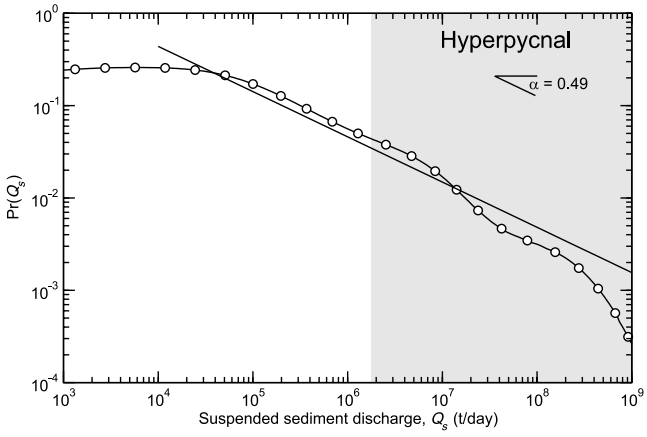

Figure 5. Magnitude-frequency distribution of suspended sediment concentration in Choshui River. Above the cutoff at 10,000 t d^{-1} the sediment discharges exhibit power law magnitude-frequency scaling with exponent, $\alpha = 0.49$. The shaded region indicates the range of hyperpycnal flows based on a critical suspended sediment concentration of 40 kg m^{-3} and the rating curve given in the text. Correctly normalized, Figure 5 would show the probability density, with an identical exponent.

[29] In order to compute the relative proportions of suspended sediment delivered under different sediment concentration conditions it is necessary to calculate the expected value of the suspended sediment discharge distribution. Since this entails calculation of the integral of the probability distribution of suspended sediment discharge, minimum and maximum sediment discharges, $Q_s^{\max} \gg Q_s^{\min}$, must be defined. The numerical values and geomorphic significance of these numbers will be discussed later. The probability distribution of suspended sediment discharge must be rescaled to give the truncated distribution, $\tilde{p}(Q_s)$, such that

$$\int_{Q_s^{\min}}^{Q_s^{\max}} \tilde{p}(Q_s)dQ_s = 1 \tag{4}$$

$$\tilde{p}(Q_s) = \frac{\alpha Q_s^{-\alpha-1}}{(Q_s^{\min})^{-\alpha} - (Q_s^{\max})^{-\alpha}}. \tag{5}$$

The expected value of suspended sediment discharge, $E(Q_s)$, is therefore

$$E(Q_s) = \int_{Q_s^{\min}}^{Q_s^{\max}} Q_s \tilde{p}(Q_s)dQ_s \tag{6}$$

$$E(Q_s) = \frac{\alpha}{1-\alpha}\left[\frac{(Q_s^{\max})^{1-\alpha} - (Q_s^{\min})^{1-\alpha}}{(Q_s^{\min})^{-\alpha} - (Q_s^{\max})^{-\alpha}}\right]. \tag{7}$$

[30] If C^* is the critical sediment concentration at which the flow becomes hyperpycnal, then Q^* is the critical water discharge at which the critical concentration is obtained. These two quantities are uniquely related by the suspended sediment rating curve (equation (1)), so that

$$C^* = \kappa (Q^*)^b, \text{ or} \tag{8}$$

$$Q^* = \left(\frac{C^*}{\kappa}\right)^{\frac{1}{b}}, \tag{9}$$

where κ is the unit sediment concentration and b is the exponent in the sediment concentration rating curve. Accordingly, the critical sediment discharge at which the flow becomes hyperpycnal, Q_s^*, is also uniquely determined, and can be written

$$Q_s^* = Q^* C^* \tag{10}$$

$$Q_s^* = \left[\frac{(C^*)^{1+b}}{\kappa}\right]^{1/b}. \tag{11}$$

It should be noted that our use of a suspended sediment rating curve in this analysis is unavoidable since no other relation between water discharge and sediment concentration is available. In view of the findings that were reported in section 6, we proceed with caution, noting that the rating curve can often lead to underestimates of hyperpycnal river discharges in Taiwan. The quantity of ultimate interest is the relative proportion of sediment discharge that is delivered when $C > C^*$, or alternatively when $Q_s > Q^*_s$. To calculate this, it is necessary to compute the expected values of Q_s

Table 3. Values of α for Hyperpycnal Rivers in Taiwan Estimated Using the Maximum Likelihood Method

Watershed	Station Number	α	Min Q_s,[a] t d^{-1}	Max Q_s,[b] t d^{-1}
Fengshan	1290H002	0.44	3×10^1	9.8×10^5
Taan	1400H009	0.36	1×10^2	1.1×10^7
Tachia	1420H035	0.80	6×10^3	2.9×10^5
Choshui	1510H058	0.49	1×10^4	3.4×10^7
Pachang	1580H005	0.60	1×10^4	6.2×10^6
Tsengwen	1630H010	0.30	1×10^3	5.8×10^6
Erhjen	1660H009	0.23	1×10^2	1.9×10^7
Peinan	2200H011	0.28	3×10^2	2.6×10^7
Hsiukuluan	2370H017	0.40	3×10^3	9.6×10^6
Hualien	2420H024	0.47	1×10^4	3.3×10^6
Hoping	2500H003	0.47	1×10^3	1.4×10^7
Lanyang	2560H006	0.33	1×10^2	5.5×10^6

[a]Min Q_s is the minimum sediment discharge for which the power law is valid.
[b]Max Q_s is the maximum recorded sediment discharge.

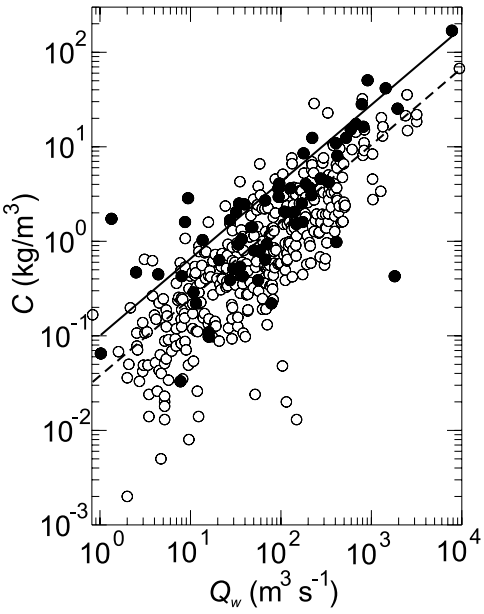

Figure 6. Suspended-sediment rating curve for Choshui River. Open circles show measurements made before Chi-Chi earthquake; solid symbols show measurements after earthquake. Dashed line is power law function of $C = \kappa_{pre} Q^b$ fitted to preearthquake data using log-transformed least squares regression; solid line is power law functions $C = \kappa_{post} Q^b$ fitted only to postearthquake data; $b = 0.82$.

between (#1) Q_s^{min} and Q_s^*, and (#2) Q_s^* and Q_s^{max}, which are

$$(\#1) = \int_{Q_s^{min}}^{Q_s^*} Q_s \tilde{p}(Q_s) dQ_s \tag{12}$$

$$(\#1) = \frac{\alpha}{1-\alpha}\left[\frac{(Q_s^*)^{1-\alpha} - (Q_s^{min})^{1-\alpha}}{(Q_s^{min})^{-\alpha} - (Q_s^{max})^{-\alpha}}\right], \tag{13}$$

$$(\#2) = \int_{Q_s^*}^{Q_s^{max}} Q_s \tilde{p}(Q_s) dQ_s \tag{14}$$

$$(\#2) = \frac{\alpha}{1-\alpha}\left[\frac{(Q_s^{max})^{1-\alpha} - (Q_s^*)^{1-\alpha}}{(Q_s^{min})^{-\alpha} - (Q_s^{max})^{-\alpha}}\right]. \tag{15}$$

For $0 < \alpha < 1$, the proportion of sediment discharge at hyperpycnal concentrations, ξ, is given as

$$\xi = \frac{(\#2)}{(\#1) + (\#2)} = 1 - \left(\frac{Q_s^*}{Q_s^{max}}\right)^{1-\alpha}. \tag{16}$$

Substituting equation (11) into equation (16) and using a similar argument to write $Q_s^{max} = [(C^{max})^{1+b}/\kappa]^{1/b}$ gives

$$\xi = 1 - \left(\frac{C^*}{C^{max}}\right)^{\frac{(1+b)(1-\alpha)}{b}}. \tag{17}$$

in which b is the suspended sediment rating curve exponent, and α is the scaling exponent of the daily suspended sediment discharge probability distribution. For constant α, the proportion of sediment discharge delivered at hyperpycnal concentrations increases as the rating curve exponent, b, increases between 0 and 1 (because $0 < C^*/C^{max} < 1$). This finding is reasonable because the rating curve exponent controls the rate of change of sediment concentration with discharge. For $b > 1$, the hyperpycnal proportion, ξ, decreases as the rating curve exponent increases; only four coastal rivers in Taiwan have $b > 1$. The hyperpycnal proportion is independent of the unit sediment concentration, κ. This is to be expected because an increase in κ, such as that observed after the Chi-Chi earthquake [*Dadson et al.*, 2004], will drive a proportionate increase in both the hyperpycnal sediment discharge and the total sediment discharge. As the magnitude-frequency scaling exponent, α, decreases there are relatively more large events, and the hyperpycnal proportion increases. Typical values are $b \approx 1$ [*Dadson*, 2004] and $\alpha \approx 0.3$–0.6 (one standard deviation range, Table 3). In the Choshui River, $b = 0.80$ and $\alpha = 0.49$.

[31] The value of C^* ($\approx$40 kg m^{-3}) is set by the physical properties of the ambient fluid [*Mulder and Syvitski*, 1995]. The most troublesome unknown in equation (17) is C^{max}. A value may be assigned to this constant either by taking it to be the largest observed value or alternatively using some theoretical maximum. The largest observed values of C^{max} in the Choshui River were 67.3 kg m^{-3} during Typhoon Herb in 1996 and 169.0 kg m^{-3} during Typhoon Toraji in 2001, after the Chi-Chi earthquake. These values, together with those for b, α given above give long-term hyperpycnal proportions, for the Choshui River, of 46% and 81%, respectively. These proportions are higher than those calculated empirically, because the present calculation is extrapolated to include all events up to the size of the Toraji flood. The maximum 24-hour rainfall during Typhoon Toraji was approximately 1 m. This amount is just over half of the maximum 24-hour rainfall during Typhoon Herb, which was 1.8 m [*Wu and Kuo*, 1999] but Toraji caused much higher suspended sediment concentrations because of increased coseismic and postseismic mass wasting in the Choshui catchment [*Dadson et al.*, 2004].

[32] Typical values of $b \approx 1$ and $\alpha \approx 0.3$–0.6 suggest an upper bound of between 80 and 94% on the proportion of hyperpycnal suspended sediment discharge from Taiwan to the ocean. The difference between this upper bound and the 30–42% hyperpycnal discharge measured between 1970 and 1999 indicates that over timescales longer than 30 years hyperpycnal discharges contribute the vast majority of sediment delivered to the ocean from Taiwan, mainly during rare, extremely large floods.

8. Events

[33] Hyperpycnal flows occur mainly during storms. We consider the effect of two typhoon storms, Herb and Toraji, which affected the Choshui River in 1996 and 2001 respectively. During Typhoon Herb the Choshui River discharged an estimated 68 Mt of suspended sediment to the ocean; during Typhoon Toraji the Choshui River discharged 175 Mt of suspended sediment to the ocean.

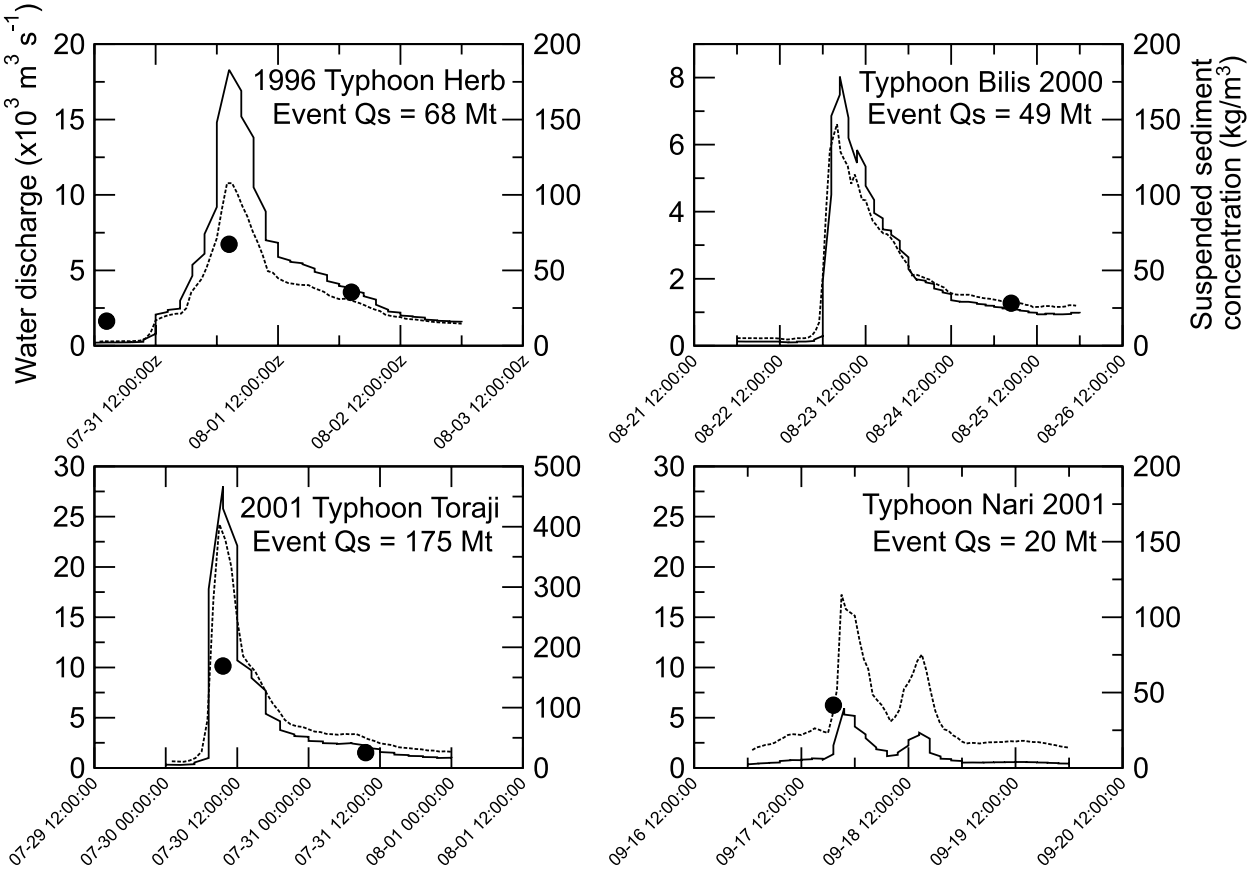

Figure 7. Hourly discharge data for recent large typhoons in Choshui River basin. Solid lines indicate water discharge, dashed lines indicate suspended sediment discharge predicted using the rating curve described in the text. Circles indicate measurements of suspended sediment concentration. Sediment discharges integrated for each event were computed using the rating curve as described in the text.

[34] During the intervening period between typhoons Herb and Toraji, the M_w 7.6 Chi-Chi earthquake occurred on the Chelungpu thrust fault. The Chi-Chi earthquake was the largest in Taiwan for 50 yr and the largest on the Chelungpu thrust for 300–620 yr [*Shin and Teng*, 2001; *Chen et al.*, 2001]. The earthquake had a reverse fault mechanism, a focal depth of 8 km, and resulted from the rupture of a ~100 km segment of the north trending, east dipping (~30°) Chelungpu thrust.

[35] Rating curves between water discharge and suspended sediment load from before and after the Chi-Chi earthquake show a factor of 2–4 increase in river sediment concentration for a given discharge (Figure 6). Moreover, the earthquake drove a 2.6-fold increase in suspended sediment discharge to the ocean from the epicentral Choshui catchment [*Dadson et al.*, 2004]. Increases in sediment discharge were driven by increases in unit sediment concentration that resulted from sediment supply during coseismic and postseismic mass wasting. This has caused changes in the magnitude and frequency of hyperpycnal flows in the Choshui River. We focus on the Choshui River because it is the river that was most affected by the Chi-Chi earthquake and is therefore the river that is most likely to have transmitted information on the geomorphic impact of the earthquake to depositional ocean environments.

[36] As noted above, calculations based on intermittent measurements and rating curve extrapolations based on daily water discharge are known to be biased downward. The former bias is because not all events are measured and those events that are measured may not be recorded

Table 4. Sediment Discharges Calculated From Hourly Data During Large Typhoons in the Choshui River Basin

Typhoon	Date	Q_{avg}, $m^3\ s^{-1}$	Q_{max}, $m^3\ s^{-1}$	Peak C_s, kg m^{-3}	Total Q_s (D),[a] Mt	Total Q_s (H),[b] Mt
Herb	31 Jul 1996	9,420	14,800	67.3	57	68
Bilis	22 Aug 2000	4,850	8,030	28.2[c]	49	49
Toraji	30 Jul 2001	7,790	28,000	169	106	175
Nari	17 Sep 2001	2,610	5,930	41.6	19	20

[a]D is computed using daily discharge data.
[b]H is computed using hourly discharge data.
[c]Concentration was measured on a different day to peak discharge.

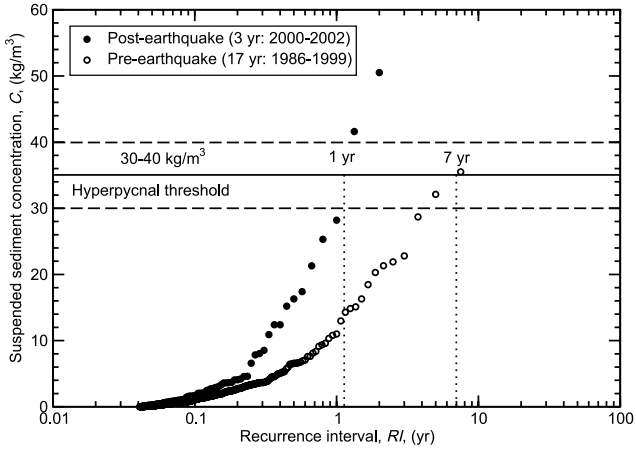

Figure 8. Change in recurrence interval of hyperpycnal discharge in Choshui River following the Chi-Chi earthquake. Open circles indicate observations before the Chi-Chi earthquake; solid circles indicate observations after the earthquake.

throughout their entire duration; the latter bias is because daily water discharge data smooth out much of the hourly discharge variability. An alternative approach is to use hourly data together with a suspended sediment concentration rating curve to calculate sediment loads associated with individual events. This approach was adopted for four typhoons; the hourly discharge data are shown in Figure 7.

[37] Application of the appropriate rating curve (pre-Chi-Chi to Herb; post-Chi-Chi to Bilis, Toraji, and Nari) gives the sediment discharges listed in Table 4. Adding to these values the nontyphoon sediment discharge (36.6 Mt, which was estimated from daily rather than hourly data) gives a total postearthquake sediment discharge in the Choshui River of 326 Mt over 680 days (1.86 years), or an annual average of 175 Mt yr^{-1}. This amount is 3 times the annual suspended sediment discharge recorded during the period before the earthquake. Of this amount, 67% was delivered at hyperpycnal concentrations.

[38] Figure 8 shows the recurrence interval for observed sediment concentration in the Choshui River before and after the Chi-Chi earthquake. Before the Chi-Chi earthquake (1986–1999), the recurrence interval for a hyperpycnal flow in the Choshui River was about 7 years, a value typical of the high-yielding rivers of eastern and southwestern Taiwan (see Figure 4). In contrast, after the Chi-Chi earthquake the recurrence interval changed to about 1 year. This earthquake-induced change was exacerbated by the greater incidence of typhoons after the earthquake. The implication of more frequent hyperpycnal flows is that more turbidites will be deposited. This is important because it may provide a recognizable stratigraphic indicator of elevated tectonic activity [e.g., *Winkler and Gawenda*, 1999]. Changes in sediment concentration caused by increased coseismic sediment supply may lead to an increase in the rate of turbidite deposition. Hyperpycnal sediment delivery almost always coincides with large typhoons, but the threshold water discharge required to produce a hyperpycnal flow is increased by coseismic changes in sediment supply and can produce larger, more frequent turbidites.

9. Conclusions

[39] In summary, during the period 1970–1999 between 99 and 115 Mt yr^{-1} of sediment was discharged at hyperpycnal sediment concentrations from Taiwan rivers to the sea. This amount represents 30–42% of the total sediment discharge from Taiwan to the ocean. The rivers with the highest overall rate of suspended sediment discharge to the ocean were Peinan, Choshui, and Kaoping. The rivers that discharged the most sediment at hyperpycnal sediment concentrations were Erhjen, Choshui, and Peinan. The rivers that delivered the greatest proportion of their load at hyperpycnal concentrations were Hoping, Erhjen, Tachia, and Choshui. A simple stochastic model shows that the long-term hyperpycnal proportion depends on α, which represents storminess, and b, which is the rating curve exponent. Following the Chi-Chi earthquake, the frequency of hyperpycnal flows increased, because earthquake-driven sediment supply increased the amount of suspended sediment transported by a given discharge [*Dadson et al.*, 2004], and therefore decreased the threshold water discharge for generating hyperpycnal flows. This finding implies that earthquakes may be recorded in sedimentary deposits as bundles of hemipelagites, hemiturbidites, and turbidites. Changes in the magnitude and frequency of the thickness of resulting turbidites may therefore provide valuable information on past changes in sediment supply.

[40] **Acknowledgments.** This work was supported by the UK Natural Environment Research Council with a CASE addition from Faber Maunsell plc, the Taiwan National Science Council, the Royal Society, and the European Union (EVG1-CT-2001-00046). Lucy Ramsey and Dimitri Lague produced Figure 1b using software written by Philippe Davy. We thank Colin Stark and John Haines for useful discussion of the mathematics and T. Mulder and an anonymous reviewer for constructive reviews.

References

Bates, C. C. (1953), Rational theory of delta formation, *AAPG Bull.*, *37*(9), 2119–2162.

Boggs, S. (1974), Sand wave fields in the Taiwan Strait, *Geology*, *2*, 251–253.

Boggs, S., W. C. Wang, F. S. Lewis, and J. C. Chen (1979), Sediment properties and water characteristics of the Taiwan shelf and slope, *Acta Oceanogr. Taiwanica*, *10*, 10–49.

Chen, W. F. (1998), Gamma-log trend facies in the Choshui Fan-delta, Taiwan, *Terr. Atmos. Oceanic Sci.*, *9*, 633–642.

Chen, W. S., Y. G. Chen, H. C. Chang, Y. H. Lee, and J. C. Lee (2001), Palaeoseismic study of the Chelungpu fault in the Wanfung area, *Western Pac. Earth Sci.*, *1*, 499–506.

Cohn, T. A. (1995), Recent advances in statistical methods for the estimation of sediment and nutrient transport in rivers, *Rev. Geophys.*, *33*, 1117–1124. (Available at http://www.agu.org/journals/rg/rg9504S/95RG00292/index.html)

Dade, W. B., and H. E. Huppert (1994), Predicting the geometry of channelized deep-sea turbidites, *Geology*, *22*, 645–648.

Dade, W. B., and H. E. Huppert (1995), Runout and fine-sediment deposits of axisymmetric turbidity currents, *J. Geophys. Res.*, *100*(C9), 18,597–18,609.

Dadson, S. J. (2004), Erosion of an active mountain belt, Ph.D. thesis, Univ. of Cambridge, Cambridge, U.K.

Dadson, S. J., et al. (2003), Links between erosion, runoff variability and seismicity in the Taiwan orogen, *Nature*, *426*, 648–651.

Dadson, S. J., et al. (2004), Earthquake-driven increase in sediment delivery from an active mountain belt, *Geology*, *32*(8), 733–736.

Hartshorn, K., N. Hovius, W. B. Dade, and R. L. Slingerland (2002), Climate-driven bedrock incision in an active mountain belt, *Science*, *297*, 2036–2038.

Hovius, N., and M. Leeder (1998), Clastic sediment supply to basins, *Basin Res.*, *10*, 1–5.

Hovius, N., C. P. Stark, H. T. Chu, and J. C. Lin (2000), Supply and removal of sediment in a landslide-dominated mountain belt: Central Range, Taiwan, *J. Geol.*, *108*, 73–89.

Lin, A. T., and A. B. Watts (2002), Origin of the West Taiwan basin by orogenic loading and flexure of a rifted continental margin, *J. Geophys. Res.*, *107*(B9), 2185, doi:10.1029/2001JB000669.

Lin, C. W., C. L. Shieh, B. D. Yuan, Y. C. Shieh, S. H. Liu, and S. Y. Lee (2004), Impact of the Chi-Chi earthquake on the occurrence of landslides and debris flows: Example from the Chenyulan River watershed, *Eng. Geol.*, *71*, 49–61.

Lin, Y. L., D. B. Ensley, S. Chiao, and C. Y. Huang (2002), Orographic influences on rainfall and track deflection associated with the passage of a tropical cyclone, *Mon. Weather Rev.*, *130*(12), 2929–2950.

Liu, C. S., S. Y. Liu, S. E. Lallemand, N. Lundberg, and D. Reed (1998), Digital elevation model offshore Taiwan and its tectonic implications, *Terr. Atmos. Oceanic Sci.*, *9*, 705–738.

Malavieille, J., et al. (2002), Arc-continent collision in Taiwan: New marine observations and tectonic evolution, in *Geology and Geophysics of an Arc-Continent Collision, Taiwan*, edited by T. B. Byrne and C. S. Liu, *Spec. Pap. Geol. Soc. Am.*, *358*, 189–213.

Milliman, J. D., and S. J. Kao (2005), Hyperpycnal discharge of fluvial sediment to the ocean: Impact of Super-Typhoon Herb (1996) on Taiwanese Rivers, *J. Geol.*, *113*, 503–506.

Milliman, J. D., and J. P. M. Syvitski (1992), Geomorphic/tectonic control of sediment discharge to the ocean: The importance of small mountain rivers, *J. Geol.*, *100*, 525–544.

Mulder, T., and J. P. M. Syvitski (1995), Turbidity currents generated at river mouths during exceptional discharges to the world oceans, *J. Geol.*, *103*, 285–299.

Mulder, T., S. Migeon, B. Savoye, and J. M. Jouanneau (2001), Twentieth century floods recorded in the deep sea Mediterranean sediment, *Geology*, *29*, 1011–1014.

Parsons, J. D., J. W. M. Bush, and J. P. M. Syvitski (2001), Hyperpycnal plume formation from riverine outflows with small sediment concentrations, *Sedimentology*, *48*, 465–478.

Shin, T. C., and T. L. Teng (2001), An overview of the 1999 Chi-Chi, Taiwan, earthquake, *Bull. Seismol. Soc. Am.*, *91*, 895–913.

Stow, D. A. V., and A. Wetzel (1990), Hemiturbidite: A new type of deep-water sediment, *Proc. Ocean Drill. Program Sci. Results*, *116*, 25–34.

Warrick, J. A., and J. D. Milliman (2003), Hyperpycnal sediment discharge from semiarid southern California rivers: Implications for coastal sediment budgets, *Geology*, *31*, 781–784.

Water Resources Agency of Taiwan (1970–2003), *Hydrological Yearbook of Taiwan*, Water Resour. Agency, Taipei, Taiwan.

Winkler, W., and P. Gawenda (1999), Distinguishing climatic and tectonic forcing of turbidite sedimentation, and the bearing on turbidite bed scaling: Palaeocene–Eocene of northern Spain, *J. Geol. Soc. London*, *156*, 791–800.

Wolman, M. G., and J. P. Miller (1960), Magnitude and frequency of geomorphic processes, *J. Geol.*, *68*, 54–74.

Wu, C. C., and Y. H. Kuo (1999), Typhoons affecting Taiwan: Current understanding and future challenges, *Bull. Am. Meteorol. Soc.*, *80*, 67–80.

Yu, H. S., C. S. Huang, and J. W. Ku (1991), Morphology and possible origin of the Kaoping submarine canyon head off south-west Taiwan, *Acta Oceanogr. Taiwanica*, *27*, 40–50.

Yu, S. B., H. Y. Chen, and L. C. Kuo (1997), Velocity field of GPS stations in the Taiwan area, *Tectonophysics*, *274*, 41–59.

H. Chen, Department of Geoscience, National Taiwan University, No. 1, Sec. 4, Roosevelt Road, Taipei, Taiwan 106.

W. B. Dade, Department of Earth Sciences, Dartmouth College, Hanover, NH 03755, USA.

S. Dadson, Centre for Ecology and Hydrology, Maclean Building, Crowmarsh Gifford, Wallingford, Oxfordshire OX10 8BB, UK. (sjdad@ceh.ac.uk)

M. J. Horng, Water Resources Agency, Ministry of Economic Affairs, Sec 3, Hsin-Yi Road, Taipei, Taiwan 106.

N. Hovius and S. Pegg, Department of Earth Sciences, University of Cambridge, Downing Street, Cambridge, CB2 3EQ, UK.

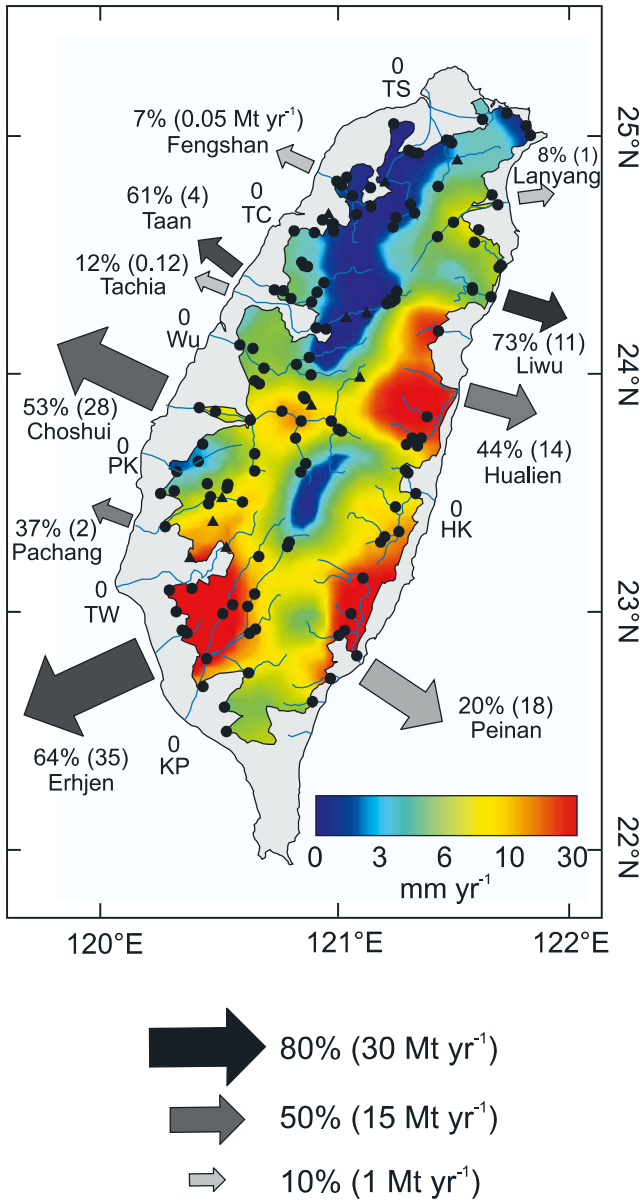

Figure 3. Hyperpycnal discharges to the ocean from Taiwan 1970–1998 based on measured hydrometric data. The map shows decadal average erosion rates for reference [from *Dadson et al.*, 2003]. Arrows indicate rivers for which at least one hyperpycnal discharge was measured (Table 1). The size of each arrow is proportional to the annual average hyperpycnal sediment discharge to the ocean (also given in parentheses); its shade is proportional to the percentage that the hyperpycnal amount represents of the total annual sediment discharge (see legend). These estimates are probably conservative, because they are based on measured data only. River names are given beneath arrows. Rivers labeled "0" had no recorded hyperpycnal sediment discharge between 1970 and 1998. The names of these rivers are abbreviated as follows: TS, Tanshui; TC, Touchien; PK, Peikang; TW, Tsengwen; KP, Kaoping; and HK, Hsiukuluan. Circles indicate hydrometric stations used to construct the erosion map; triangles indicate locations of water supply reservoirs. No data are available in the outermost light grey area.